



THE UNIVERSITY *of* EDINBURGH

Edinburgh Research Explorer

Molecular subclasses of clear cell ovarian carcinoma and their impact on disease behavior and outcomes

Citation for published version:

Bolton, KL, Chen, D, Corona De La Fuente, RI, Fu, Z, Murali, R, Kbel, M, Tazi, Y, Cunningham, JM, Chan, ICC, Wiley, BJ, Moukarzel, LA, Winham, SJ, Armasu, SM, Lester, J, Elishaev, E, Laslavic, A, Kennedy, CJ, Piskorz, A, Sekowska, M, Brand, AH, Chiew, Y, Pharoah, P, Elias, KM, Drapkin, R, Churchman, M, Gourley, C, Defazio, A, Karlan, B, Brenton, JD, Weigelt, B, Anglesio, MS, Huntsman, D, Gayther, SA, Konner, J, Modugno, F, Lawrenson, K, Goode, EL & Papaemmanuil, E 2022, 'Molecular subclasses of clear cell ovarian carcinoma and their impact on disease behavior and outcomes', *Clinical Cancer Research*.
<https://doi.org/10.1158/1078-0432.CCR-21-3817>

Digital Object Identifier (DOI):

[10.1158/1078-0432.CCR-21-3817](https://doi.org/10.1158/1078-0432.CCR-21-3817)

Link:

[Link to publication record in Edinburgh Research Explorer](#)

Document Version:

Peer reviewed version

Published In:

Clinical Cancer Research

Publisher Rights Statement:

This work is licensed under a Creative Commons Attribution-NonCommercial-NoDerivatives 4.0 International License .

<https://doi.org/10.1158/1078-0432.CCR-21-3817>

General rights

Copyright for the publications made accessible via the Edinburgh Research Explorer is retained by the author(s) and / or other copyright owners and it is a condition of accessing these publications that users recognise and abide by the legal requirements associated with these rights.

Take down policy

The University of Edinburgh has made every reasonable effort to ensure that Edinburgh Research Explorer content complies with UK legislation. If you believe that the public display of this file breaches copyright please contact openaccess@ed.ac.uk providing details, and we will remove access to the work immediately and investigate your claim.



1 **Molecular subclasses of clear cell ovarian carcinoma and their impact on disease behavior and** 2 **outcomes**

3
4 Kelly L Bolton^{1*}, Denise Chen^{2*}, Rosario Corona de la Fuente^{3*}, Zhuxuan Fu^{4*}, Rajmohan Murali^{5*},
5 Martin Köbel^{6*}, Yanis Tazi^{5*}, Julie M. Cunningham^{7*}, Irenaeus C.C. Chan¹, Brian J. Wiley¹, Lea A.
6 Moukarzel^{5*}, Stacey J. Winham⁷, Sebastian M. Armasu⁷, Jenny Lester⁸, Esther Elishaev⁴, Angela
7 Laslavic⁴, Catherine J. Kennedy^{9,10}, Anna Piskorz¹¹, Magdalena Sekowska¹¹, Alison H. Brand^{9,12}, Yoke-
8 Eng Chiew^{9,10}, Paul Pharoah¹¹, Kevin M. Elias¹³, Ronny Drapkin¹⁴, Michael Churchman¹⁵, Charlie
9 Gourley¹⁵, Anna DeFazio^{9,10,12,16}, Beth Karlan⁸, James D. Brenton¹¹, Britta Weigelt⁵, Michael S.
10 Anglesio¹⁷, David Huntsman¹⁷, Simon Gayther^{3*}, Jason Konner^{5*}, Francesmary Modugno^{4*}, Kate
11 Lawrenson^{3*}, Ellen L. Goode^{7*}, Elli Papaemmanuil^{5*}

12
13 ¹Washington University School of Medicine, St Louis MO, USA; ²Philadelphia College of Osteopathic
14 Medicine, Philadelphia, PA; ³Cedars-Sinai Medical Center, Los Angeles, CA, USA; ⁴University of
15 Pittsburgh Graduate School of Public Health, Pittsburgh, PA, USA; ⁵Memorial Sloan-Kettering Cancer
16 Center, New York, NY, USA; ⁶The University of Calgary, Calgary, Canada; ⁷Mayo Clinic, Rochester,
17 MN, USA; ⁸David Geffen School of Medicine, Department of Obstetrics and Gynecology, University of
18 California at Los Angeles, Los Angeles, CA, USA; ⁹Department of Gynaecological Oncology,
19 Westmead Hospital, Sydney, New South Wales, Australia; ¹⁰Centre for Cancer Research, The
20 Westmead Institute for Medical Research, Sydney, New South Wales, Australia; ¹¹University of
21 Cambridge, Cambridge, UK; ¹²The University of Sydney, Sydney, New South Wales, Australia;
22 ¹³Brigham and Women's Hospital, Boston, MA, USA; ¹⁴University of Pennsylvania, Philadelphia, PA,
23 USA; ¹⁵University of Edinburgh, Edinburgh, UK; ¹⁶The Daffodil Centre, The University of Sydney, a joint
24 venture with Cancer Council NSW, Sydney, New South Wales, Australia; ¹⁷University of British
25 Columbia, Vancouver, BC, Canada.

26
27 Running Title: Molecular subclasses of clear cell ovarian carcinoma

28
29
30 *Denotes equal contribution

31
32 Correspondence to be addressed to:
33 Kelly L. Bolton
34 bolton@wustl.edu
35 Washington University, St Louis MO
36

37 **Conflict of Interest**

38 KLB receives grant funding from Bristol Myers Squibb and Servier, outside the scope of this study. BW
39 reports ad hoc membership of the advisory board of Repare Therapeutics, outside the scope of this
40 study. ADeF has received grant funding and honoraria from AstraZeneca, outside the scope of this
41 study.

42 **Statement of translational relevance**

43 Clear cell ovarian cancer (CCOC) is the second most common subtype of epithelial ovarian cancer and
44 when diagnosed at an advanced stage has a poor prognosis. The relationship between molecular
45 profiles and clinical presentation or outcomes are still unknown but could help guide the development of
46 personalized therapeutic approaches for CCOC. Here we profiled 421 primary CCOCs using deep
47 targeted sequencing and whole transcriptome sequencing on a subset of 211. Clustering of cancer
48 driver mutations and RNA expression converged upon two distinct subclasses of CCOC. The first was
49 dominated by *ARID1A*-mutated tumors with enriched expression of canonical CCOC genes and
50 markers of platinum resistance; the second was largely comprised of tumors with *TP53*-mutations and
51 enriched for the expression of genes involved in extracellular matrix organization and mesenchymal
52 differentiation. These two distinct molecular subclasses showed distinct clinical presentation and
53 outcomes, with potential relevance to therapeutic responsiveness.

54

55 **Abstract**

56
57 **Purpose:** To identify molecular subclasses of clear cell ovarian carcinoma (CCOC) and assess their
58 impact on clinical presentation and outcomes.

59
60 **Experimental Design:** We profiled 421 primary CCOCs that passed quality control using a targeted
61 deep sequencing panel of 163 putative CCOC driver genes and whole transcriptome sequencing of 211
62 of these tumors. Molecularly-defined subgroups were identified and tested for association with clinical
63 characteristics and overall survival.

64
65 **Results:** We detected a putative somatic driver mutation in at least one candidate gene in 95% (401
66 out of 421) of CCOC tumors including: *ARID1A* (in 49% of tumors), *PIK3CA* (49%), *TERT* (20%) and
67 *TP53* (16%). Clustering of cancer driver mutations and RNA expression converged upon two distinct
68 subclasses of CCOC. The first was dominated by *ARID1A*-mutated tumors with enriched expression of
69 canonical CCOC genes and markers of platinum resistance; the second was largely comprised of
70 tumors with *TP53*-mutations and enriched for the expression of genes involved in extracellular matrix
71 organization and mesenchymal differentiation. Compared to the *ARID1A*-mutated group, women with
72 *TP53*-mutated tumors were more likely to have advanced stage disease, no antecedent history of
73 endometriosis, and poorer survival, driven by their advanced stage at presentation. In women with
74 *ARID1A*-mutated tumors, there was a trend towards lower response rate to first-line platinum-based
75 therapy.

76
77 **Conclusions:** Our study suggests that CCOC consists of two distinct molecular subclasses with
78 distinct clinical presentation and outcomes, with potential relevance to both traditional and experimental
79 therapy responsiveness.

80

81

82 **Introduction**

83 Historically, tumor treatment approaches have been dictated by tissue site; but large-scale molecular
84 profiling efforts have shown that remarkable heterogeneity exists in the landscape of cancer driver
85 genes and pathways within tumor types and even within histologic subtypes. This has been well
86 characterized for many common tumors through multi-omic profiling¹ and characterization of the
87 genetic determinants of tumor behavior and outcome has led to the development of personalized
88 therapeutic approaches. Indeed, for some cancers, prognosis and therapeutic strategies are based
89 primarily on their presence of genetic driver mutations identified in the tumor²⁻⁷. For several rare cancer
90 types such as ovarian clear cell carcinoma (CCOC), no strong associations between molecular profiles
91 and clinical presentation or outcomes are known and broad-acting platinum-based chemotherapy
92 remains the standard of care.

93 When diagnosed at an advanced stage, CCOC has a worse outcome than other invasive ovarian
94 cancers including the more common high-grade serous ovarian carcinoma (HGSOC) (median overall
95 survival of 10 months)^{8,9}, presents at a younger age¹⁰, and is less responsive to platinum-based
96 therapy¹¹. Relatively small studies suggest that CCOC possesses several driver events that are distinct
97 from HGSOC. CCOC is thought to arise from endometriotic lesions with recurrent somatic mutations in
98 *PIK3CA* and *ARID1A*, which are rare in HGSOC¹²⁻¹⁵. In addition, the existing data suggests that
99 CCOCs are commonly *TP53*-wild-type (whereas HGSOC ubiquitously harbors *TP53* mutations) and
100 exhibits fewer structural rearrangements than HGSOC¹³. However, it is not known whether clinically
101 meaningful molecular subtypes of CCOC exist.

102 In the current study, we performed comprehensive targeted sequencing and transcriptomic profiling of a
103 large, multi-ethnic cohort of 421 primary CCOCs to identify disease subclasses with distinct biology and
104 clinical behavior, which-in turn may provide avenues for personalized therapeutic approaches.

105 **Materials and Methods**

106 *Study Participants*

107 Clinical data and therapy-naïve fresh frozen tumor material were utilized from women diagnosed with
108 invasive CCOC and enrolled into research studies from the following sites: Memorial Sloan Kettering
109 Cancer Center Gynecology Tissue Bank (MSK; New York NY, USA), Mayo Clinic (MAY; Rochester
110 MN, USA), Addenbrooks Hospital (ADD; England), Cedars-Sinai Medical Center (WCP; Los Angeles
111 CA, USA), University of Pittsburgh (PIT; Pittsburgh PA, USA), Gynaecological Oncology Biobank
112 (GynBiobank) at Westmead Hospital (WMH; Sydney, Australia), University of Edinburgh (SCOT;
113 Scotland), Canadian Ovarian Experimental Unified Resource (COEUR; Multiple sites, Canada),
114 Brigham and Women's Hospital (BWH; Boston MA, USA), and University of Pennsylvania (UPA;
115 Philadelphia PA, USA). Participants provided written informed consent. The studies were conducted in
116 accordance with recognized ethical guidelines (e.g., Declaration of Helsinki, CIOMS, Belmont Report,
117 U.S. Common Rule), and approved by local institutional review boards. Extraction of DNA/RNA was
118 performed centrally at MSK (for cases from MSK, WCP, PIT, BWH and UPA) or locally (for cases
119 from MAY, ADD, WMH and COEUR). For the cases which were extracted centrally at MSK, slides
120 from frozen tissue sections were reviewed by a pathologist (R.M) and extraction of DNA/RNA was
121 performed from tumor sections, selected based on high content (>80%) of clear cell carcinoma. In total,
122 tumors from 447 women diagnosed with CCOC were analyzed. Race and menstruation status (pre vs.
123 post-menopausal) was obtained through participant self-report. History of endometriosis was also
124 obtained through self-report except at MSK where endometriosis was only available if mentioned on the
125 pathology report. Tumor characteristics and clinical outcomes were obtained through medical record
126 review.

127 *Targeted DNA Sequencing and Analysis-*

128 We performed targeted sequencing of 163 putative CCOC driver genes (Supplementary Table 1) in
129 DNA samples from the 447 tumor and blood-derived DNA from 16 unmatched controls using a custom
130 Nimblegen capture-based panel. Genes were selected based on a combined analysis of 105 clear cell
131 somatic sequencing studies including: (1) whole genome sequencing of 31 CCOCs from Wang et al.¹³;

132 (2) whole exome sequencing of eight cases from Jones et al¹²; (3) targeted sequencing of 26 CCOCs
133 using a panel of 465 known cancer drivers (MSK-IMPACT)¹⁶; and targeted or whole exome sequencing
134 of 40 CCOCs from project GENIE¹⁷. Included in our panel were 119 genes where somatic mutations
135 have been identified in two or more CCOCs; 41 established cancer driver genes based on the COSMIC
136 Cancer Gene Census¹⁸ mutated in one CCOC and three genes in the SWI/SNF complex (*SMARCB1*,
137 *SMARCC1*, *SMARCC2*)¹⁴ that have been implicated in CCOC biology¹⁹ (Supplementary Table 1). We
138 also included on the sequencing panel highly polymorphic single nucleotide variants distributed every
139 3MB throughout the genome to capture large copy number deletions/amplifications.

140 Of 447 tumor samples, 421 (94%) passed quality control. As a technical set of normal samples (panel
141 of normals), we included DNA extracted from the blood of ten healthy, cancer free individuals. Two
142 tumor samples failed due to low coverage, 12 due to sample contamination and 12 due to duplication.
143 The median sequencing coverage per sample was 539x. Raw sequence data were aligned to the
144 human genome (NCBI build 37) using BWA²⁰. Variant calling for single nucleotide variants was
145 performed using Mutect2²¹, Strelka²² and CaVEMan²³ and for insertions/deletions using Pindel²⁴,
146 Mutect2²¹ and Strelka²². We considered mutations to be true if they: (1) passed at least two variant
147 callers; (2) were present at a variant allele fraction of greater than 2%; (3) were present in gNOMAD²⁵
148 whole exome sequencing data with a maximum population frequency of less than 0.001; (4) had a
149 variant allele frequency (VAF) at least two times greater than the median VAF in a panel of normal
150 samples; and (5) were present in none of the panel of normal samples at a VAF of 2% or greater. We
151 further excluded mutations in low complexity regions (DUST²⁶ score >7). Mutations in known cancer
152 hotspots that met all other requirements but failed due to low complexity or to only being passed by one
153 variant caller were retained for consideration. We calculated a microsatellite instability score for each
154 tumor using MSI sensor²⁷

155 We used Bayesian Dirichlet processes to establish classification rules that partitioned tumors into
156 subgroups, minimizing overlap between categories. The Dirichlet process defines an infinite prior
157 distribution for the number and proportions of clusters in a mixture model, fitted with the use of the
158 Markov chain Monte Carlo method²⁸. Our method was based on an implementation of the Dirichlet

159 process mixture model available at <https://github.com/nicolaroberts/hdp> using a non-hierarchical
160 Dirichlet process. We used 5,000 burnin iterations and subsequently sampled 10,000 realizations at
161 intervals of 20 iterations. From this collection of data, we computed the optimal number of clusters,
162 requiring that 90% of the samples were assigned a cluster.

163 *Whole Transcriptome Sequencing and Analysis*

164 RNA-Seq libraries were prepared for 211 cases from total RNA derived from the same tumor section
165 using poly(A) enrichment of the mRNA. 100 bp paired-end libraries were sequenced on Illumina's
166 HiSeq at a targeted depth of 40 million reads per sample. We performed alignment using STAR²⁹
167 (version STAR_2.5.1b) against the reference genome hg38 (GENCODE v26). Reads were summarized
168 using featureCounts³⁰ (version 1.5.0-p1). RNA clusters were defined using hierarchical clustering using
169 the top 500 most variable protein coding genes (clustering parameters: method = ward.D2, distance =
170 canberra). Differentially expressed genes between RNA cluster 1 and RNA cluster 2 samples were
171 obtained using the R package DESeq2³¹ (version 1.28.1) with collection site and RNA cluster as part of
172 the design formula. Pathway enrichment analysis was performed using Metascape⁴ (version 3.5),
173 looking for enrichment of GO and KEGG terms, Hallmark, Reactome and BioCarta Gene Sets, and
174 Canonical Pathways. The top 500 most overexpressed genes in RNA cluster 1 (\log_2 fold change < 1
175 and FDR < 0.05) and the top 500 most overexpressed genes in RNA cluster 2 were used as input for
176 Metascape³².

177 *Outcome Analyses*

178 Survival data was available for 350 cases. Survival time was calculated from the date of diagnosis to
179 last follow-up and allowed for left truncation for cases who were consented following diagnosis. We
180 right censored at five years from diagnosis to reduce non-ovarian cancer related deaths. Race, age at
181 diagnosis (continuous and quadratic, assigned as site median for three cases), tumor stage, extent of
182 residual disease and study site were considered as covariates using a Cox Proportional Hazards
183 model. Proportionality of hazards was examined using Schoenfeld residuals. In addition, contingency
184 analysis was done on tumor mutational status and tumor cluster with primary treatment response

185 (complete response or partial response compared to stable or progressive disease) stratified by tumor
186 stage and vital status up to five years using a chi-square test.

187 **Data Availability Statement**

188 The somatic variant calls and normalized RNAseq intensity data, code and deidentified clinical data is
189 available here: https://github.com/kbolton-lab/Bolton_OCCC . This will enable all the figures and tables
190 to be re-generated and also provide data for others for future analyses. We will also make the
191 BAMs/FASTQs available to researchers through contacting Kelly Bolton (bolton@wustl.edu).

192

193 **RESULTS**

194 *Clinical characteristics*

195 Key characteristics, other than race, of the 421 participants included in the study did not vary between
196 study sites (Table 1). Compared to clinical characteristics reported in the literature for women with
197 HGSOC^{10,33}, women with CCOC in this cohort were more likely to be of Asian ancestry (12% of
198 individuals with non-missing race), have a history of endometriosis (13%) and present with early stage
199 disease (69%).

200 *Targeted DNA sequencing of candidate CCOC driver genes*

201 In 163 candidate CCOC driver genes we identified 6,361 mutations. Of these, 1,488 mutations were
202 classified as potentially pathogenic based upon annotation in OncoKB³⁴, frequency in COSMIC,
203 frequency in previously published CCOC sequencing data^{12,13,16}, predicted pathogenicity based on
204 PolyPhen³⁵ and SIFT³⁶, and prior evidence in the literature (Supplementary Table 2). At least one
205 putative driver mutation was identified in 401 out of 421 tumors (95%) (mean number of mutations 3,
206 range 1-25) (Figure 1a and c). The most commonly mutated genes were *ARID1A* (49%, N=205),
207 *PIK3CA* (45%, N=188) and the *TERT* promoter (20%, N=84). The most frequently recurrent mutations
208 were clonally dominant with a VAF >35% (e.g. *ARID1A* and *TP53*) suggesting that they represented
209 early events while others (e.g. *CREBBP*) were more often sub-clonal, possibly representing secondary

210 events (Figure 1b). We detected a higher proportion (16%, N=71) of tumors with *TP53* mutations than
211 has been described by some (9-15%)^{13,37} but not all NGS studies (18%)³⁸. This raises the possibility
212 that some of the CCOCs in this cohort were misdiagnosed high-grade serous or endometrioid ovarian
213 cancers. We explored this possibility in detail. First, we noted that 10 out of 71 *TP53* mutations (14%)
214 were deeply sub-clonal (VAF<10%); previous studies may not have detected these mutations as they
215 used lower-depth sequencing (Figure 1b). Second, we performed additional pathologic review to verify
216 clear cell histology for a subset of the cases where formalin-fixed paraffin-embedded (FFPE) tissue
217 sections were available. This included 14 (20%) of the *TP53*-mutated cases and 4 (15%) of the
218 *BRCA1/2*-mutated cases where formalin-fixed paraffin-embedded (FFPE) tissue sections were
219 available. On the basis of morphology combined with and immunohistochemical staining of Napsin A,
220 p53, and WT1³⁹ (markers of HGSOC and not CCOC) it was determined that four out of 14 *TP53*-mutant
221 cases (28%) (three endometrioid carcinomas and one HGSOC) were misclassified as CCOC. None of
222 the *BRCA1/2*-mutated cases were misclassified. Thus, by extrapolation we estimate that approximately
223 19 of our 71 *TP53*-mutant tumors in this cohort were misclassified.

224 A subset of tumors (N=20) bore mutations in *SMARCA4*, a gene that is the sole driver mutation in
225 ovarian small cell carcinoma hypercalcemic type (OSCCHT)⁴⁰⁻⁴². However, unlike OSCCHT, in our
226 CCOC cases we observed *SMARCA4* to be most commonly co-mutated with either *ARID1A* (50%) or
227 *PIK3CA* (35%). Similar to our analysis of *TP53* mutated cases we performed central pathology review
228 of a subset (N=8) of the *SMARCA4* mutated cases. All of these cases showed typical CCOC
229 morphology and were positive for clear cell markers such as PAX8 (8/8 diffuse), and Napsin A (5/8
230 diffuse, 2/8 focal) or HNF1B (5/5 diffuse). We conclude that there was no evidence for these cases
231 being misclassified OSCCHT. Whether *SMARCA4* has a similar driver capacity in CCOC compared to
232 OSCCHT requires further study.

233
234 Most cases (75%) had at least one large-scale copy number event with the most frequently recurrent
235 events reflecting common cancer-driver aneuploidies including 8q amplification¹⁹ (Supplementary
236 Figure 1). Cases with *TP53* mutations had more whole chromosome or arm-level aneuploidies (mean
237 =12) compared to wild-type tumors (mean = 8) (Supplementary Figure 2). *TP53*-mutant/*ARID1A*-mutant

238 tumors showed less genomic instability (mean number of aneuploidies=7) compared to *TP53*-
239 mutant/*ARID1A*-wildtype tumors (mean number of aneuploidies=13). We detected recurrent fusions in
240 *TGM7* (N=5) as previously shown by Earp *et al*⁴³. In addition, recurrent fusions involving *BCAR4* (N=6),
241 *ITCH* (N=6) and *DCAF12* (N=5) were observed. These are known cancer fusion partners but have not
242 been reported in CCOC before. (Supplementary Figure 3).

243 We evaluated mutation status with respect to clinical and epidemiological factors including age, race,
244 tumor and history of endometriosis. Compared to *ARID1A*-mutated tumors, patients with *KRAS*
245 mutations were older at presentation (median age 53 vs. 67, $p=0.03$; Figure 2a). Individuals with a
246 history of endometriosis were more likely to have *ARID1A*-mutated tumors (72% and 47% of patients
247 with and without endometriosis respectively, $p=2 \times 10^{-4}$) (Figure 2b). Advanced stage tumors were more
248 likely to harbor *TP53* mutations than early-stage tumors (27% vs. 11% respectively, $p=2 \times 10^{-4}$) (Figure
249 2c). Among *TP53* mutant tumors, a similar proportion (50% and 51%, respectively) were advanced
250 stage with or without co-occurring *ARID1A* mutations. There was a trend towards a higher frequency of
251 *ARID1A*-mutated tumors in women of east Asian descent but this was not significant (Figure 2d).

252 We next examined the relationship between mutational burden, cancer driver genes and patterns of
253 genetic co-occurrence. Several genes harbored recurrent mutations within the same tumor
254 (Supplementary Figure 4). This seen for both tumor suppressor genes (e.g. *ARID1A*) and specific
255 oncogenes including *PIK3R1* and *PIK3CA*. Among tumors with multiple *PIK3CA* mutations, variants
256 were more likely to occur in non-hotspot locations within the gene (Supplementary Figure 5)⁴⁴.
257 MSIsensor score was higher among individuals more than 10 driver mutations (N=12, 3%) and among
258 those with *MSH2* and *MSH6* mutations (Supplementary Figure 6). We observed a statistically
259 significant co-occurrence between mutations in *ARID1A*, *PIK3CA*, *TP53* and *BRCA1/BRCA2* Mutual
260 exclusivity between somatic mutations of *ARID1A*, *TP53*, *PIK3CA* and *PIK3R1* (Supplementary Figure
261 7) suggests that these may represent distinct pathways to oncogenesis. The exclusivity between *TP53*
262 and *ARID1A* mutation was stronger in the setting of multiple *ARID1A* mutations (OR=0.21; 95% CI
263 0.07-0.54, $p=2 \times 10^{-4}$) compared to a single *ARID1A* mutations (OR=0.68, 95% CI 0.32-1.34, $p=0.28$).
264 “We observed 54 mutations in genes known to be relevant to high penetrance genetic predisposition to

265 ovarian cancer including *PMS2*, *MSH6*, *MSH2*, *BRCA1* and *BRCA2*. Overall 52% of these mutations
266 were present at a VAF in the tumor of $\geq 35\%$. In the absence of matched normal tissue sequencing,
267 we were not able to distinguish these from germline variants. Thus, it is possible that up to 26 cases
268 (6% of the cohort) harbored a germline pathogenic variant in a known cancer susceptibility gene.”

269 Because we observed clear patterns of exclusivity and co-occurrence between gene drivers, we used
270 unsupervised clustering approaches to define non-overlapping subgroups of CCOC based on their
271 mutational spectrum. We defined seven subgroups (Supplementary Figure 8) and compared the
272 frequency of mutations between subgroups. Four clusters were characterized by having an *ARID1A*
273 mutation; the first cluster (cluster A) was characterized by a single *ARID1A* mutation in combination
274 with another disease defining mutation (e.g. *PIK3CA*, *TERT*, *TP53*, *KRAS*, *PTEN*, *PPP2R1A*, *PIK3R1*,
275 *CREBBP* or *SPOP*) (N=86); the second (cluster B) with a single *ARID1A* mutation alone or in
276 combination with non-disease defining mutation (N=19); the third (cluster C) with multiple *ARID1A*
277 mutations combined with a *PIK3CA* mutation (N=81); and a fourth (cluster D) with multiple *ARID1A*
278 mutations and *PIK3CA* wild-type (N=25). Two clusters were *ARID1A* wildtype: Cluster E was defined by
279 a *TP53* mutation (N=50); and cluster F by other non-*TP53* disease-defining mutations (N=104). A final
280 cluster (cluster G) was characterized by mutations in *SMARCA4* (N=13); a mutation typically observed
281 in small cell ovarian carcinoma²³. The remaining tumors were undefined (N=57).

282 Similar to the patterns we observed when studying the association between individual mutations and
283 clinical features, the *TP53*-mutated, *ARID1A*-wild-type cluster showed an enrichment of advanced
284 stage disease while tumors belonging to the *ARID1A*-mutant clusters were more likely in individuals of
285 Asian ancestry and those with a history of endometriosis (Supplementary Figure 9). Individuals in
286 cluster G (*SMARCA4*-mutant tumors) had a non-significant trend towards a younger age at diagnosis
287 ($p=0.32$).

288 *Transcriptomic profiling of CCOC*

289 Transcriptomic profiles were generated for 212 CCOC tumors in which targeted sequencing was also
290 performed. Using unsupervised clustering informed by expression of the 500 most variable genes, we

291 identified two main RNA clusters (Supplementary Figure 10): Expression cluster 1 showed higher
292 expression of genes previously reported as highly expressed in CCOC including *ANXA4* and *GPX3*,
293 both of which are linked to platinum resistance^{45,46}. Among the most highly expressed genes in cluster
294 1 compared to 2 also included *GPX3*^{4,7}, which is known to be overexpressed in endometriosis
295 compared to normal endometrial tissue, and *EEF1A2*, known to be overexpressed in CCOC associated
296 endometriosis but not benign endometriosis⁴⁸. Genes that characterized this cluster were enriched in
297 metabolic pathways including flavonoid glucuronidation ($p=10^{-15}$) and monocarboxylic acid metabolism
298 ($p=10^{-13}$). Expression cluster 2 showed enriched expression of genes involved in extracellular matrix
299 (ECM) organization ($p=10^{-22}$) and mesenchymal differentiation, including genes such as *ADGR2* and
300 *PDCH19* (Supplementary Figure 10 and Figure 3b). Compared to cluster 1, expression cluster 2 also
301 showed higher expression of *WT1* and lower expression of CCOC marker *HNF1B*, which are features
302 classically associated with high-grade serous ovarian cancer⁹ (Figure 3b). Expression cluster 2 was
303 enriched with *TP53*-mutant tumors (55% of cases in cluster 2 compared to 10% in cluster 1). When
304 comparing RNA expression and mutation clusters, cluster 2 was largely comprised of tumors belonging
305 to mutation cluster E i.e *TP53*-mutant *ARID1A*-wildtype tumors (45% of cluster 2) and the undefined
306 mutation cluster (33% of cluster 2) (Figure 3a).⁷

307 *Clinical Outcomes*

308 There was no statistically significant association between overall survival and CCOC mutations when
309 examined on a per-gene level in Cox proportional hazards models stratified by study site
310 (Supplementary Table 3). We observed a non-significant trend towards improved survival for patients
311 with *ARID1A* (HR=0.82, 95% CI 0.58-1.15, $p=0.24$) and *PTEN* (HR=0.52, 95% CI 0.24-1.12, $p=0.10$)
312 mutant tumors. Because of the similarity of the *ARID1A*-mutant clusters in regards to clinical
313 presentation and outcome, we combined these clusters for the purpose of survival analysis. Women
314 with *TP53*-mutant, *ARID1A*-wildtype tumors had worse overall survival compared to those with
315 *ARID1A*-mutant tumors (HR=1.72, 95% CI 1.06-2.81, $p=0.03$, Figure 4a). Similarly, RNAseq cluster 2
316 showed an increased risk of death compared to RNAseq cluster 1 (Figure 4b, Tumor Cluster 2 versus
317 Tumor Cluster 1 HR 2.8, 95% CI 1.66 – 4.84; $p=1 \times 10^{-4}$). Covariate adjustment for age, race, stage and

318 residual disease attenuated the estimated mutation and cluster-associated risk (Supplementary Table
319 4). To explore how these subgroups might influence therapy outcome, we studied the relationship
320 between mutation status and response to first line therapy with platinum/taxane combination therapy.
321 We limited this to women with advanced stage disease who successfully underwent debulking surgery
322 followed by combination platinum/taxol therapy (N=36). Women with *ARID1A* wild-type, *TP53*-mutant
323 tumors were more likely to have a complete response 75% (N=11) compared to *ARID1A*-mutant tumors
324 (55%), although this was not statistically significant (p=0.33) in this small sample size.

325 **DISCUSSION**

326 Our results have several clinical implications. First, the results of both genomic and transcriptomic
327 cluster associations with clinical presentation and outcome converged, suggesting two main subgroups
328 of CCOC: The first subtype included *ARID1A*-mutant tumors (particularly double-mutant tumors) and
329 other common CCOC mutations (e.g. *PIK3CA*, *TERT* etc) that showed enriched expression of
330 metabolic pathways, presented with early stage disease and were more likely to have a history of
331 endometriosis. We denote this group as “classic-CCOC”, which represented 83% of our cohort. The
332 second CCOC subtype was dominated by *TP53*-mutant tumors that showed enriched expression of
333 genes involved in extracellular matrix organization, mesenchymal differentiation and immune-related
334 pathways. These cases presented with advanced disease and had worse survival. Interestingly, *TP53*
335 mutations either in the presence or absence of co-occurring *ARID1A* mutations were associated with a
336 higher degree of genomic instability and aggressive, advanced stage tumors. The worse survival for
337 tumors in this “HGSOC-like” subgroup was largely explained by advanced stage and higher burdens of
338 residual disease.

339 Within both the “classic-CCOC” and “HGSOC-like” subgroups we noted a subset of individuals had
340 tumor with mutations in genes known to be both somatic drivers of ovarian cancer and germline
341 susceptibility genes including *PMS2*, *MSH6*, *MSH2*, *BRCA1*, and *BRCA2*. Due to the absence of
342 matched normal samples, we were unable to fully distinguish whether these represented somatic or
343 germline events and is a limitation of our study. Future studies estimating the frequency of CCOC

344 cases that arise in women with strong hereditary predisposition and who may be considered for risk
345 reducing bilateral salpingo-oophorectomy should be prioritized⁴⁹.

346 There is increasing recognition that other histological types of ovarian carcinoma, including HGSOE
347 and endometrioid carcinoma, can contain areas with clear cell change complicating the histologic
348 diagnosis⁵⁰. While a subset of cases in the “HGSOE-like” cluster are misclassified HGSOE, and is a
349 weakness of our study, it is unlikely that this alone explains our findings. Firstly, all of our cases were
350 morphologically diagnosed by expert gynecological pathologists and at some centers, this morphologic
351 review was supplemented by immunohistochemistry for histotype-specific markers. Secondly, in a
352 subset of *TP53*-mutant cases, we re-confirmed the diagnosis of CCOC using a combination of
353 morphological and immunohistochemical features. Thus, our results suggest that a subset of *bona fide*
354 CCOCs with HGSOE-like features exist. Our results also emphasize that expert histologic review of
355 CCOC cases, particularly those who present with *TP53*-mutant, *ARID1A*-wildtype tumors, is warranted
356 given similarities to the biology and behavior of HGSOE.

357 Gene expression profiles of the “classic-CCOC” and “HGSOE-like” CCOC subtypes we observed are
358 similar to those reported by Tan et al.⁵¹ which also reported two clusters, the first enriched for genes in
359 metabolic pathways and the second, a less common mesenchymal-like subgroup associated with late-
360 stage disease. However, unlike Tan et al., we observed differences in the frequency of *TP53*-mutated
361 tumors across clusters. The source of this discrepancy is unclear and may include differences in
362 sequencing technology (Tan et al. performed targeted sequencing using Ion Torrent) and patient
363 characteristics (Tan et al., included only women of Asian ancestry which trend towards lower
364 frequencies of *TP53*-mutated tumors in our analysis and which are known to have lower frequencies of
365 endometrial ovarian cancer). The overlap between genes highly expressed in our “classic-CCOC”
366 subgroup and those enriched in endometriosis provide further support for the likely transition from
367 endometriosis to carcinoma in CCOC.

368 The greatest translational impact from these molecular CCOC subtypes is expected to lie in the
369 development of therapeutic approaches tailored to the vulnerabilities of each group. Interestingly,

370 despite being aggressive on presentation, a trend was seen towards the “HGSOC-like” CCOC
371 subgroup having higher response rates to first line platinum-based chemotherapy. Future studies are
372 warranted to further explore whether genomic subtypes of CCOC predict response to platinum-based
373 and other therapies as treatment data were limited here. The “classic-CCOC” subgroup dominated by
374 mutations in the SWI/SNF pathway and markers linked to chemo-resistance may be of particular
375 relevance to target for investigational first-line therapies. Recent data suggests that the SWI/SNF
376 pathway plays a novel role in the regulation of anti-tumor immunity, and that SWI/SNF deficiency can
377 be therapeutically targeted by immune checkpoint blockade¹⁹. Several studies are currently evaluating
378 the role of immune check point inhibitors in CCOC including NCT03405454, NCT03425565. While a
379 limitation of our study was that we were unable to assess MMR functional status, we did note a rare
380 subset of tumors (3%) with higher mutational burden (>10 drivers) and MSI sensor score. The extent to
381 which the subset of CCOCs with higher total mutation and with MMR deficiency show improved
382 responsiveness to immune checkpoint blockade in ongoing clinical trials will be an important avenue of
383 investigation. Additional targeted therapeutic strategies have been explored in preclinical settings
384 including epigenetic synthetic lethality, some of which are entering into clinical trials. The PI3K inhibitor,
385 alepelisib, is now FDA approved for HR-positive breast cancer and ongoing trials in additional *PIK3CA*-
386 mutated cancers including CCOC are underway. Double *PIK3CA* mutations appear to hyperactivate
387 PI3K signaling and enhance tumor growth and may confer increased responsiveness to PI3K inhibitors
388 than those with a single mutation⁵². Thus, for CCOC cases harboring multiple *PIK3CA* mutations, PI3K
389 inhibitors either alone or in combination with other agents may represent a promising approach.

390 The strengths of this study include the large sample size, use of multiple study sites, inclusion of
391 women of European and non-European ancestry, and integration of genetic and transcriptomic markers
392 of disease behavior and outcome. While this is the most extensive genomic study of CCOC to date,
393 greater sample size with additional follow-up data will allow improved assessment and validation of
394 these clinically relevant subtypes. Although future analyses would benefit from larger patient
395 collections, our current results suggest that genomic classification may inform the future development
396 of targeted therapeutics in CCOC.

397 **Acknowledgements**

398 Research reported in this publication was supported in part by a Cancer Center Support Grant of the
399 NIH/NCI (Grant No. P30CA008748, MSK) and the Cycle for Survival including the Fatma Fund. B.
400 Weigelt is funded in part by Breast Cancer Research Foundation and NIH/NCI (P50 CA247749 01)
401 grants. KLB is funded by the Damon Runyon Cancer Research Foundation, the American Society of
402 Hematology, the EvansMDS Foundation and the NCI (Grant 5K08CA241318). Additional support was
403 provided by R21CA222867, R01CA248288, P30CA015083, and P50CA136393. M. Anglesio was
404 funded through a Michael Smith Health Research BC Scholar Program award and the Janet D.
405 Cottrelle Foundation Scholars Program (managed by the BC Cancer Foundation). This study used
406 resources provided by the Canadian Ovarian Cancer Research Consortium's COEUR biobank funded
407 by the Terry Fox Research Institute and managed and supervised by the Centre hospitalier de
408 l'Université de Montréal. The Consortium acknowledges contributions of its COEUR biobank from
409 Institutions across Canada (for a full list see <http://www.tfri.ca/en/research/translationalresearch/coeur/>).
410 This work was supported by the Westmead Hospital Department of Gynaecological Oncology, Sydney
411 Australia. The Gynaecological Oncology Biobank at Westmead (GynBiobank), a member of the
412 Australasian Biospecimen Network-Oncology group, was funded by the National Health and Medical
413 Research Council of Australia (Enabling Grants ID 310670 & ID 628903) and the Cancer Institute NSW
414 (Grants 12/RIG/1-17 & 15/RIG/1-16). The Westmead GynBiobank acknowledges financial support from
415 the Sydney West Translational Cancer Research Centre, funded by the Cancer Institute NSW. A.
416 Piskorz, M. Sekowska, and J. Brenton were supported by Cancer Research UK grant 22905. Additional
417 support was also provided by the National Institute of Health Research (NIHR) Cambridge Biomedical
418 Research Centre (BRC-1215-20014). The views expressed are those of the authors and not
419 necessarily those of the NHS, the NIHR, or the Department of Health and Social Care.

420

421

422 REFERENCES

- 423 1. Bailey, M. H. *et al.* Comprehensive Characterization of Cancer Driver Genes and Mutations. *Cell*
424 **173**, 371-385.e18 (2018).
- 425 2. Dong, J., Li, B., Lin, D., Zhou, Q. & Huang, D. Advances in Targeted Therapy and Immunotherapy
426 for Non-small Cell Lung Cancer Based on Accurate Molecular Typing. *Front. Pharmacol.* **10**, (2019).
- 427 3. Quintás-Cardama, A., Kantarjian, H. & Cortes, J. Imatinib and beyond—exploring the full potential of
428 targeted therapy for CML. *Nat. Rev. Clin. Oncol.* **6**, 535–543 (2009).
- 429 4. Ortega, J., Vigil, C. E. & Chodkiewicz, C. Current Progress in Targeted Therapy for Colorectal
430 Cancer. *Cancer Control* **17**, 7–15 (2010).
- 431 5. Kayser, S. & Levis, M. J. Advances in targeted therapy for acute myeloid leukaemia. *Br. J. Haematol.*
432 **180**, 484–500 (2018).
- 433 6. Tangutoori, S., Baldwin, P. & Sridhar, S. PARP inhibitors: A new era of targeted therapy. *Maturitas*
434 **81**, 5–9 (2015).
- 435 7. Vaishnavi, A., Le, A. T. & Doebele, R. C. TRKking Down an Old Oncogene in a New Era of Targeted
436 Therapy. *Cancer Discov.* **5**, 25–34 (2015).
- 437 8. Lee, Y.-Y. *et al.* Prognosis of ovarian clear cell carcinoma compared to other histological subtypes: a
438 meta-analysis. *Gynecol. Oncol.* **122**, 541–547 (2011).
- 439 9. Irodi, A. *et al.* Patterns of clinicopathological features and outcome in epithelial ovarian cancer
440 patients: 35 years of prospectively collected data. *BJOG Int. J. Obstet. Gynaecol.* **127**, 1409–1420
441 (2020).
- 442 10. Wentzensen, N. *et al.* Ovarian Cancer Risk Factors by Histologic Subtype: An Analysis From
443 the Ovarian Cancer Cohort Consortium. *J. Clin. Oncol. Off. J. Am. Soc. Clin. Oncol.* **34**, 2888–2898
444 (2016).
- 445 11. Iida, Y., Okamoto, A., Hollis, R. L., Gourley, C. & Herrington, C. S. Clear cell carcinoma of the
446 ovary: a clinical and molecular perspective. *Int. J. Gynecol. Cancer* ijgc (2020) doi:10.1136/ijgc-
447 2020-001656.

- 448 12. Jones, S. *et al.* Frequent mutations of chromatin remodeling gene ARID1A in ovarian clear cell
449 carcinoma. *Science* **330**, 228–231 (2010).
- 450 13. Wang, Y. K. *et al.* Genomic consequences of aberrant DNA repair mechanisms stratify ovarian
451 cancer histotypes. *Nat. Genet.* **49**, 856–865 (2017).
- 452 14. Anglesio, M. S. *et al.* Multifocal endometriotic lesions associated with cancer are clonal and
453 carry a high mutation burden. *J. Pathol.* **236**, 201–209 (2015).
- 454 15. Murakami, R. *et al.* Exome Sequencing Landscape Analysis in Ovarian Clear Cell Carcinoma
455 Shed Light on Key Chromosomal Regions and Mutation Gene Networks. *Am. J. Pathol.* **187**, 2246–
456 2258 (2017).
- 457 16. Cheng, D. T. *et al.* Memorial Sloan Kettering-Integrated Mutation Profiling of Actionable Cancer
458 Targets (MSK-IMPACT): A Hybridization Capture-Based Next-Generation Sequencing Clinical Assay
459 for Solid Tumor Molecular Oncology. *J. Mol. Diagn. JMD* **17**, 251–264 (2015).
- 460 17. Consortium, T. A. P. G. AACR Project GENIE: Powering Precision Medicine through an
461 International Consortium. *Cancer Discov.* **7**, 818–831 (2017).
- 462 18. Sondka, Z. *et al.* The COSMIC Cancer Gene Census: describing genetic dysfunction across all
463 human cancers. *Nat. Rev. Cancer* **18**, 696–705 (2018).
- 464 19. Fukumoto, T., Magno, E. & Zhang, R. SWI/SNF Complexes in Ovarian Cancer: Mechanistic
465 Insights and Therapeutic Implications. *Mol. Cancer Res. MCR* **16**, 1819–1825 (2018).
- 466 20. Li, H. & Durbin, R. Fast and accurate short read alignment with Burrows-Wheeler transform.
467 *Bioinforma. Oxf. Engl.* **25**, 1754–1760 (2009).
- 468 21. Benjamin, D. *et al.* Calling Somatic SNVs and Indels with Mutect2. *bioRxiv* 861054 (2019)
469 doi:10.1101/861054.
- 470 22. Saunders, C. T. *et al.* Strelka: accurate somatic small-variant calling from sequenced tumor-
471 normal sample pairs. *Bioinforma. Oxf. Engl.* **28**, 1811–1817 (2012).
- 472 23. Jones, D. *et al.* cgpCaVEManWrapper: Simple Execution of CaVEMan in Order to Detect
473 Somatic Single Nucleotide Variants in NGS Data. *Curr. Protoc. Bioinforma.* **56**, 15.10.1-15.10.18
474 (2016).

- 475 24. Ye, K., Schulz, M. H., Long, Q., Apweiler, R. & Ning, Z. Pindel: a pattern growth approach to
476 detect break points of large deletions and medium sized insertions from paired-end short reads.
477 *Bioinformatics* **25**, 2865–2871 (2009).
- 478 25. Karczewski, K. J. *et al.* The mutational constraint spectrum quantified from variation in 141,456
479 humans. *Nature* **581**, 434–443 (2020).
- 480 26. Morgulis, A., Gertz, E. M., Schäffer, A. A. & Agarwala, R. A fast and symmetric DUST
481 implementation to mask low-complexity DNA sequences. *J. Comput. Biol. J. Comput. Mol. Cell Biol.*
482 **13**, 1028–1040 (2006).
- 483 27. Niu, B. *et al.* MSIsensor: microsatellite instability detection using paired tumor-normal sequence
484 data. *Bioinforma. Oxf. Engl.* **30**, 1015–1016 (2014).
- 485 28. Teh, Y. W., Jordan, M. I., Beal, M. J. & Blei, D. M. Hierarchical Dirichlet Processes. *J. Am. Stat.*
486 *Assoc.* **101**, 1566–1581 (2006).
- 487 29. Dobin, A. *et al.* STAR: ultrafast universal RNA-seq aligner. *Bioinformatics* **29**, 15–21 (2013).
- 488 30. Liao, Y., Smyth, G. K. & Shi, W. featureCounts: an efficient general purpose program for
489 assigning sequence reads to genomic features. *Bioinformatics* **30**, 923–930 (2014).
- 490 31. Love, M. I., Huber, W. & Anders, S. Moderated estimation of fold change and dispersion for
491 RNA-seq data with DESeq2. *Genome Biol.* **15**, 550 (2014).
- 492 32. Zhou, Y. *et al.* Metascape provides a biologist-oriented resource for the analysis of systems-
493 level datasets. *Nat. Commun.* **10**, 1523 (2019).
- 494 33. Lisio, M.-A., Fu, L., Goyeneche, A., Gao, Z. & Telleria, C. High-Grade Serous Ovarian Cancer:
495 Basic Sciences, Clinical and Therapeutic Standpoints. *Int. J. Mol. Sci.* **20**, 952 (2019).
- 496 34. Chakravarty, D. *et al.* OncoKB: A Precision Oncology Knowledge Base. *JCO Precis. Oncol.*
497 **2017**, (2017).
- 498 35. Adzhubei, I., Jordan, D. M. & Sunyaev, S. R. Predicting Functional Effect of Human Missense
499 Mutations Using PolyPhen-2. *Curr. Protoc. Hum. Genet. Editor. Board Jonathan Haines AI* **07**,
500 Unit7.20 (2013).

- 501 36. Ng, P. C. & Henikoff, S. SIFT: predicting amino acid changes that affect protein function.
502 *Nucleic Acids Res.* **31**, 3812–3814 (2003).
- 503 37. Kuo, K.-T. *et al.* Frequent Activating Mutations of PIK3CA in Ovarian Clear Cell Carcinoma. *Am.*
504 *J. Pathol.* **174**, 1597–1601 (2009).
- 505 38. Friedlander, M. L. *et al.* Molecular Profiling of Clear Cell Ovarian Cancers. *Int. J. Gynecol.*
506 *Cancer* **26**, 648–654 (2016).
- 507 39. Köbel, M. *et al.* An Immunohistochemical Algorithm for Ovarian Carcinoma Typing. *Int. J.*
508 *Gynecol. Pathol.* **35**, 430–441 (2016).
- 509 40. Jelinic, P. *et al.* Recurrent SMARCA4 mutations in small cell carcinoma of the ovary. *Nat.*
510 *Genet.* **46**, 424–426 (2014).
- 511 41. Ramos, P. *et al.* Small cell carcinoma of the ovary, hypercalcemic type, displays frequent
512 inactivating germline and somatic mutations in SMARCA4. *Nat. Genet.* **46**, 427–429 (2014).
- 513 42. Witkowski, L. *et al.* Germline and somatic SMARCA4 mutations characterize small cell
514 carcinoma of the ovary, hypercalcemic type. *Nat. Genet.* **46**, 438–443 (2014).
- 515 43. Earp, M. A. *et al.* Characterization of fusion genes in common and rare epithelial ovarian cancer
516 histologic subtypes. *Oncotarget* **8**, 46891–46899 (2017).
- 517 44. Saito, Y. *et al.* Landscape and function of multiple mutations within individual oncogenes.
518 *Nature* **582**, 95–99 (2020).
- 519 45. Morimoto, A. *et al.* Annexin A4 induces platinum resistance in a chloride-and calcium-dependent
520 manner. *Oncotarget* **5**, 7776–7787 (2014).
- 521 46. Y, S. *et al.* Glutathione peroxidase 3 is a candidate mechanism of anticancer drug resistance of
522 ovarian clear cell adenocarcinoma. *Oncol. Rep.* **20**, (2008).
- 523 47. Tamaresis, J. S. *et al.* Molecular Classification of Endometriosis and Disease Stage Using High-
524 Dimensional Genomic Data. *Endocrinology* **155**, 4986–4999 (2014).
- 525 48. Worley, M. J. *et al.* Molecular changes in endometriosis-associated ovarian clear cell
526 carcinoma. *Eur. J. Cancer* **51**, 1831–1842 (2015).

- 527 49. Berek, J. S. *et al.* Prophylactic and risk-reducing bilateral salpingo-oophorectomy:
528 recommendations based on risk of ovarian cancer. *Obstet. Gynecol.* **116**, 733–743 (2010).
- 529 50. DeLair, D. *et al.* HNF-1 β in Ovarian Carcinomas With Serous and Clear Cell Change. *Int. J.*
530 *Gynecol. Pathol. Off. J. Int. Soc. Gynecol. Pathol.* **32**, 541–546 (2013).
- 531 51. Tan, T. Z. *et al.* Analysis of gene expression signatures identifies prognostic and functionally
532 distinct ovarian clear cell carcinoma subtypes. *EBioMedicine* **50**, 203–210 (2019).
- 533 52. Vasan, N. *et al.* Double PIK3CA mutations in cis increase oncogenicity and sensitivity to PI3K α
534 inhibitors. *Science* **366**, 714–723 (2019).
- 535
- 536

	ADD (N=28)	BWH (N=9)	COEUR (N=181)	MAY (N=38)	MSK (N=60)	PIT (N=24)	SCOT (N=22)	UPA (N=7)	WCP (N=28)
Age(y)									
0-40	0 (0%)	0 (0%)	3 (1.7%)	1 (2.6%)	1 (1.7%)	0 (0%)	0 (0%)	0 (0%)	2 (7.1%)
40-50	1 (3.6%)	0 (0%)	37 (20.4%)	3 (7.9%)	6 (10.0%)	4 (16.7%)	4 (18.2%)	2 (28.6%)	7 (25.0%)
50-60	8 (28.6%)	2 (22.2%)	81 (44.8%)	16 (42.1%)	28 (46.7%)	9 (37.5%)	7 (31.8%)	2 (28.6%)	14 (50.0%)
60-70	13 (46.4%)	7 (77.8%)	48 (26.5%)	9 (23.7%)	19 (31.7%)	5 (20.8%)	9 (40.9%)	2 (28.6%)	4 (14.3%)
70+	6 (21.4%)	0 (0%)	11 (6.1%)	9 (23.7%)	6 (10.0%)	6 (25.0%)	2 (9.1%)	1 (14.3%)	1 (3.6%)
Missing	0 (0%)	0 (0%)	1 (0.6%)	0 (0%)	0 (0%)	0 (0%)	0 (0%)	0 (0%)	0 (0%)
Race									
White	16 (57.1%)	9 (100%)	0 (0%)	38 (100%)	44 (73.3%)	23 (95.8%)	0 (0%)	6 (85.7%)	23 (82.1%)
Asian	2 (7.1%)	0 (0%)	0 (0%)	0 (0%)	13 (21.7%)	0 (0%)	0 (0%)	0 (0%)	4 (14.3%)
Black	0 (0%)	0 (0%)	0 (0%)	0 (0%)	1 (1.7%)	1 (4.2%)	0 (0%)	1 (14.3%)	1 (3.6%)
Other	0 (0%)	0 (0%)	0 (0%)	0 (0%)	2 (3.3%)	0 (0%)	0 (0%)	0 (0%)	0 (0%)
Unknown	10 (35.7%)	0 (0%)	181 (100%)	0 (0%)	0 (0%)	0 (0%)	22 (100%)	0 (0%)	0 (0%)
Endometriosis									
yes	0 (0%)	0 (0%)	13 (7.2%)	10 (26.3%)	6 (10.0%)	0 (0%)	2 (9.1%)	2 (28.6%)	7 (25.0%)
no	0 (0%)	9 (100%)	168 (92.8%)	26 (68.4%)	49 (81.7%)	0 (0%)	20 (90.9%)	5 (71.4%)	0 (0%)
unknown	28 (100%)	0 (0%)	0 (0%)	2 (5.3%)	5 (8.3%)	24 (100%)	0 (0%)	0 (0%)	21 (75.0%)
FIGO Stage									
I/II	17 (60.7%)	7 (77.8%)	128 (70.7%)	25 (65.8%)	42 (70.0%)	16 (66.7%)	14 (63.6%)	2 (28.6%)	15 (53.6%)
III/IV	5 (17.9%)	2 (22.2%)	46 (25.4%)	12 (31.6%)	17 (28.3%)	8 (33.3%)	7 (31.8%)	5 (71.4%)	13 (46.4%)
Missing	6 (21.4%)	0 (0%)	7 (3.9%)	1 (2.6%)	1 (1.7%)	0 (0%)	1 (4.5%)	0 (0%)	0 (0%)

Table 1. Clinical Characteristics of CCOC cases sequenced using targeted panel

537
538

539

540 **Figure 1. Mutational landscape of 401 Clear Cell Ovarian Carcinomas with a Detectable**
541 **Mutation.** (a) Proportion of patients with mutations in commonly mutated genes. (b) Mutation variant
542 allele frequency (VAF) by genes mutated in at least 10% of individuals. (c) Number of mutated genes
543 per individual. (d) Variant effect and nucleotide substitution change for single nucleotide variants.

544 **Figure 2. Frequency of somatic mutations by clinical characteristics including** a) age at
545 diagnosis, b) endometriosis, c) stage and d) race. Genes that were mutated in at least 20 individuals
546 with non-missing values for the clinical characteristic were included. Shown are q-values (FDR
547 corrected p-values) based on fisher's exact test. * $q < 0.05$; ** $q < 0.01$
548

549 **Figure 3. The transcriptome of Clear Cell Ovarian Cancer Samples.** (a) Sankey plot showing the
550 correspondence of the samples annotations RNA clusters and DNA clusters. (b) Heatmap showing the
551 normalized gene expression of the top 50 most differentially expressed genes between RNA cluster 1
552 and RNA cluster 2.
553

554 **Figure 4. Association between CCOC molecular subgroups and all-cause mortality.** Shown are
555 the Kaplan Meier plots for the survival probability over five years following CCOC diagnosis stratified by
556 (a) mutational clusters defined by ARID1A/TP53 mutation status, (b) RNAseq expression clusters.
557
558

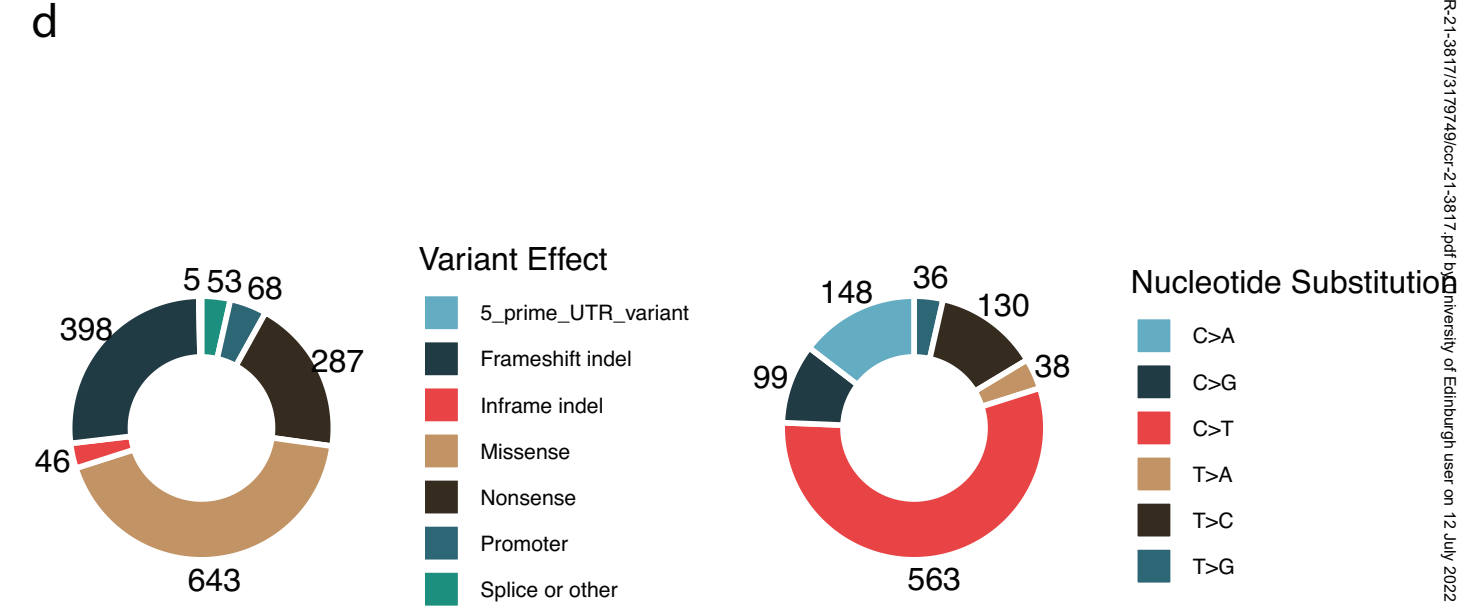
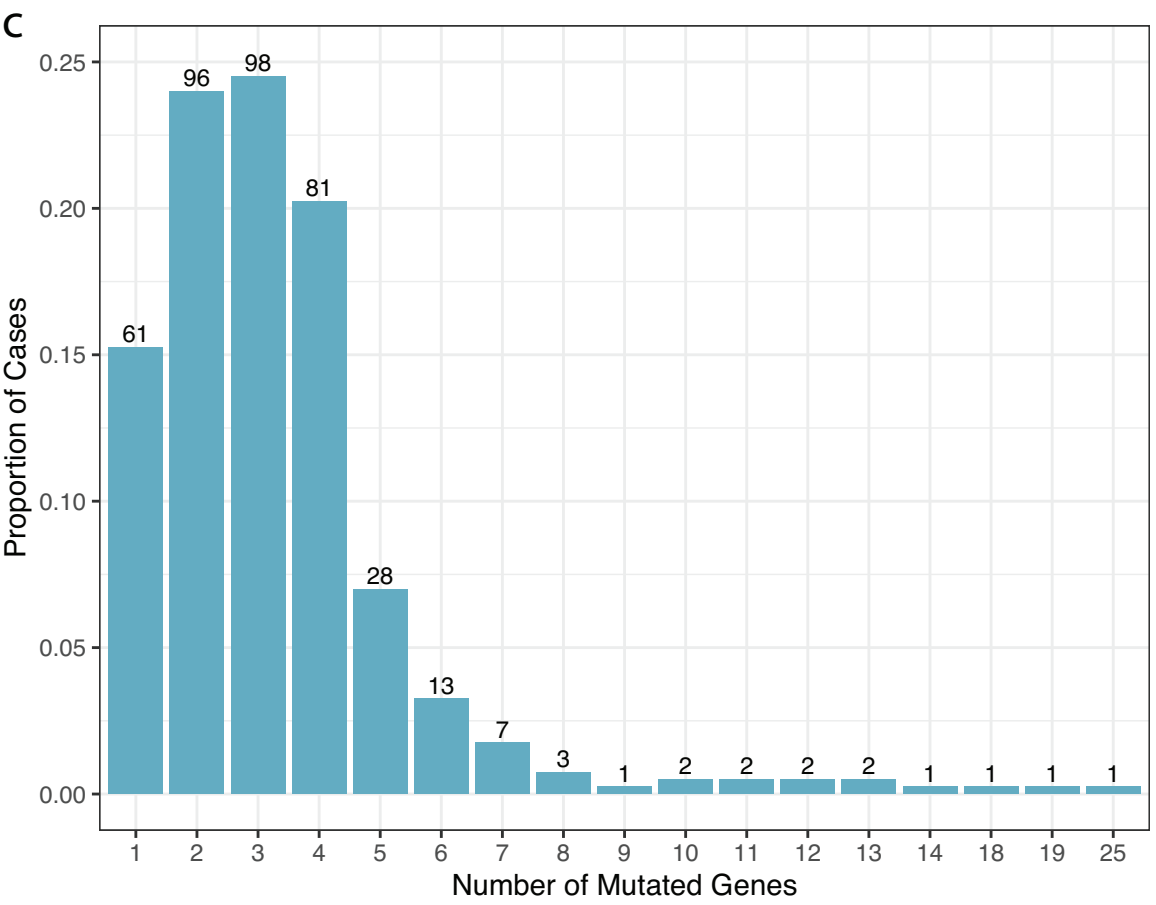
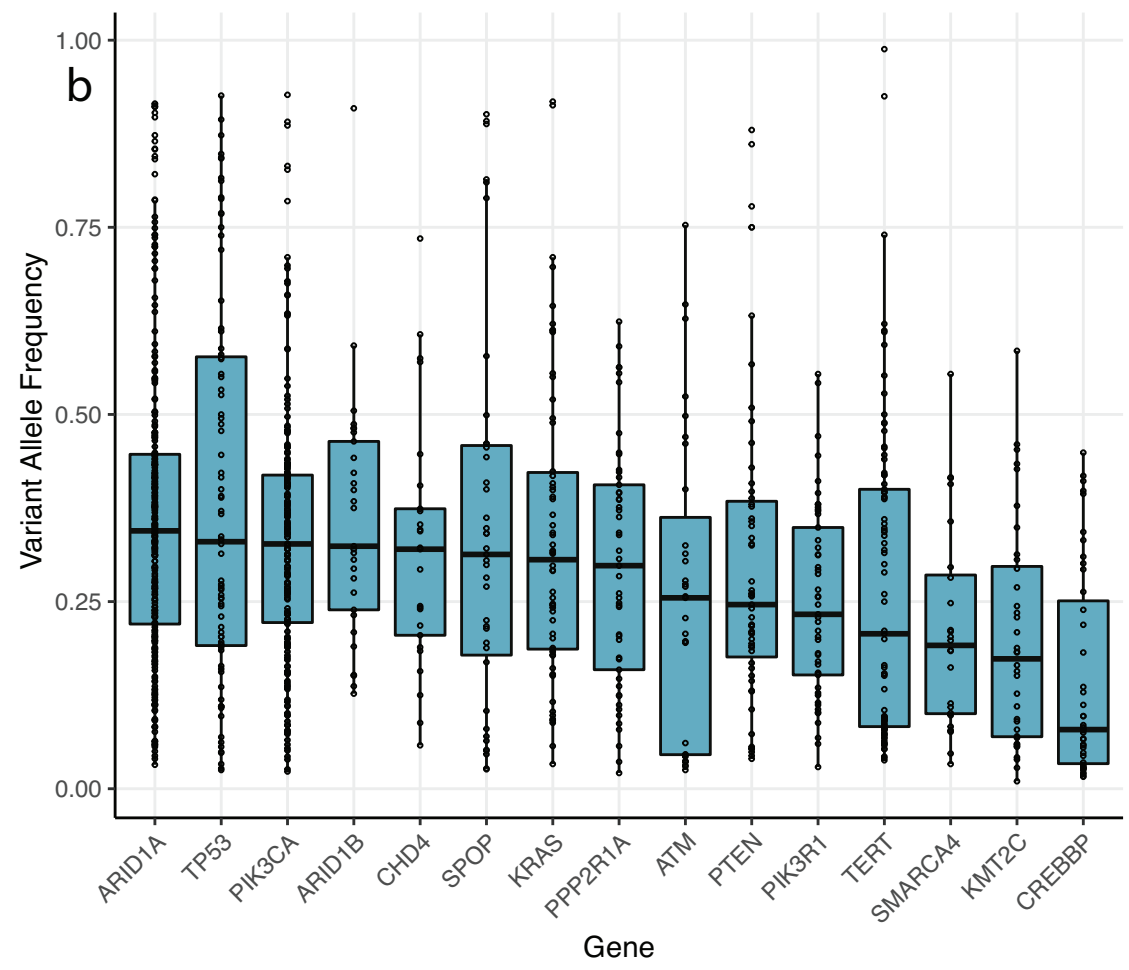
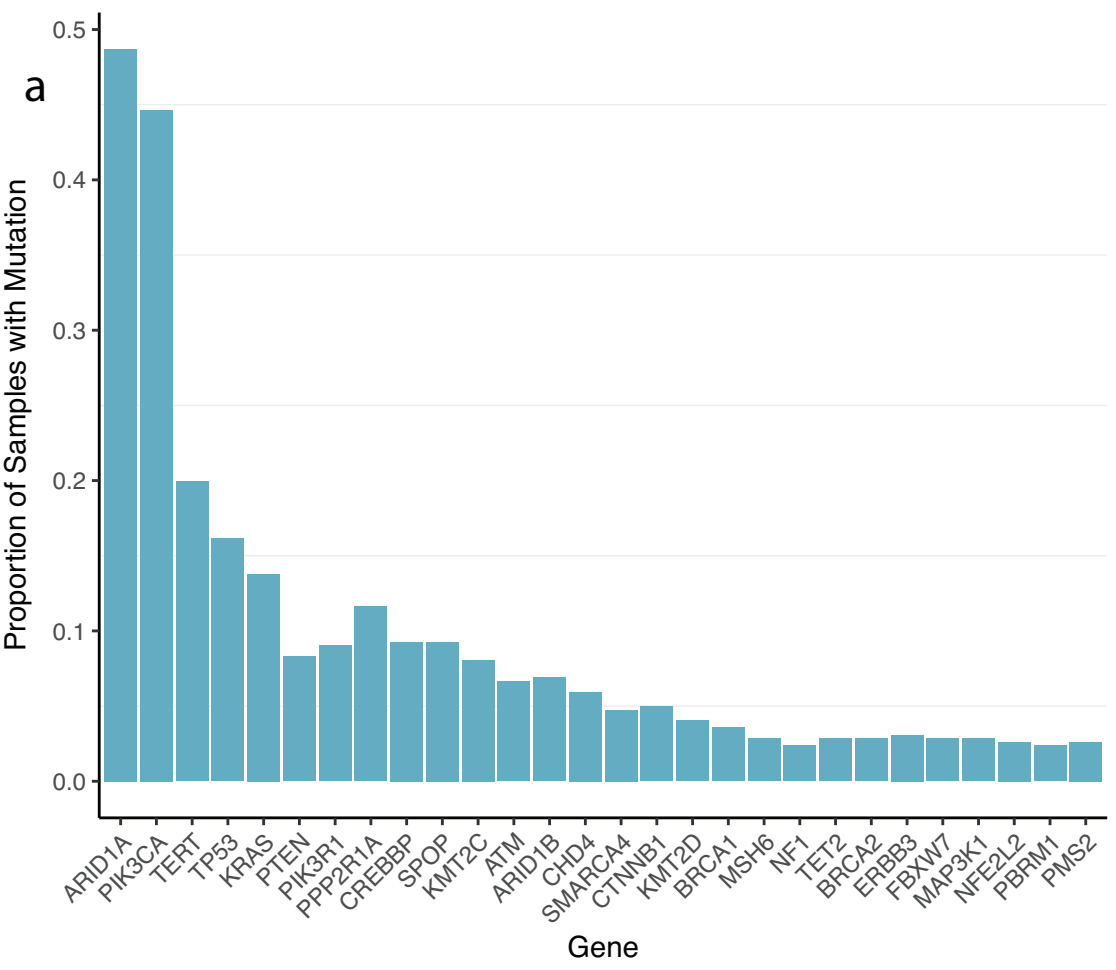


Figure 1.

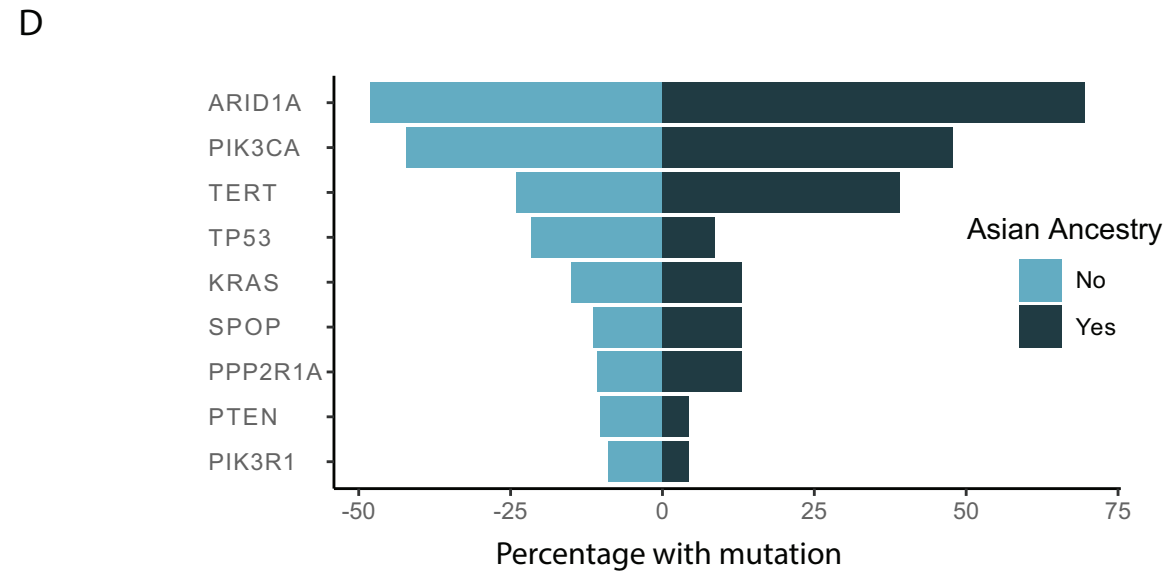
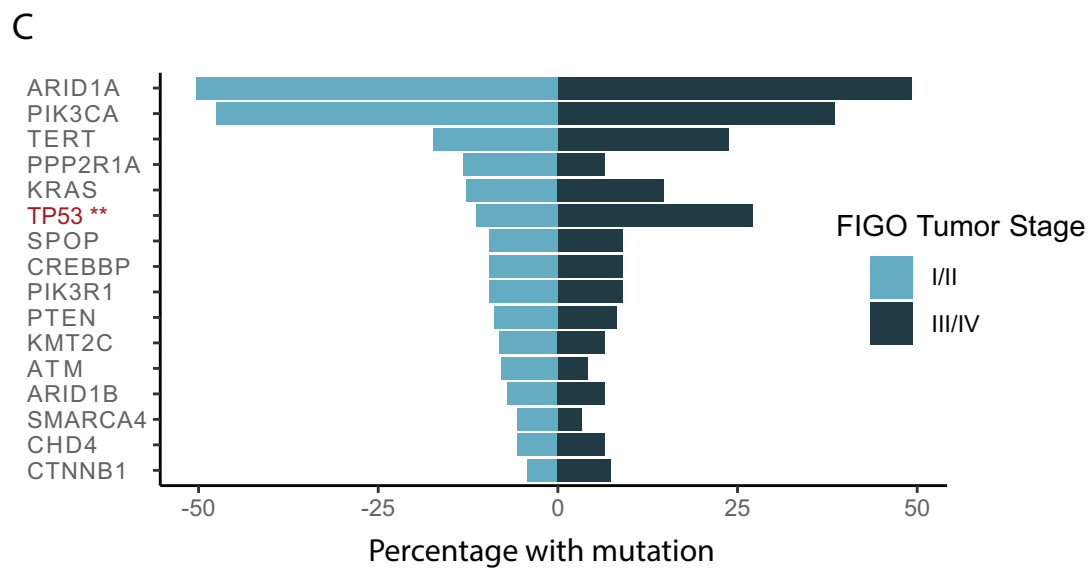
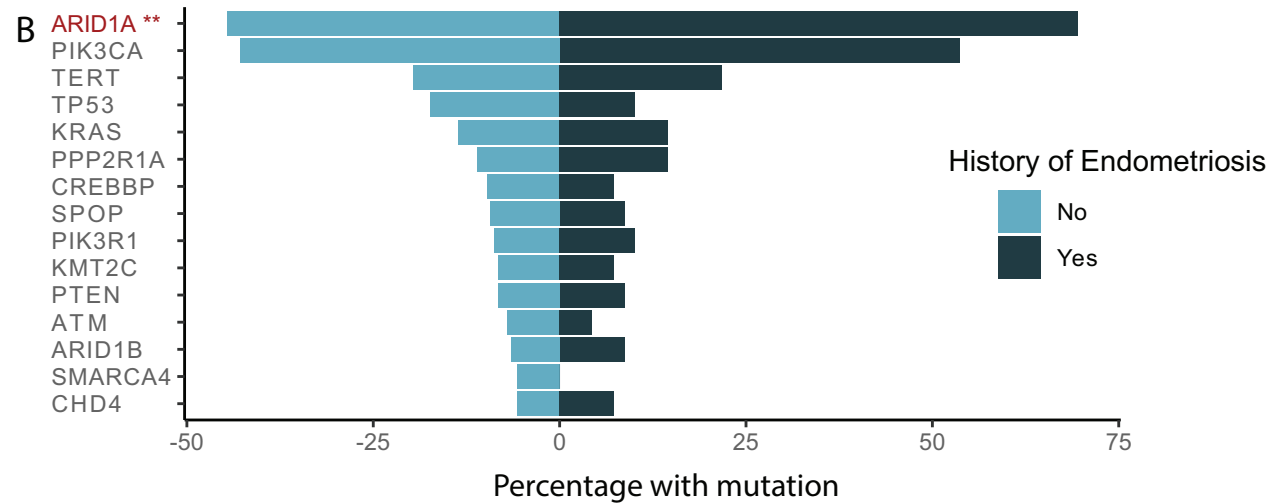
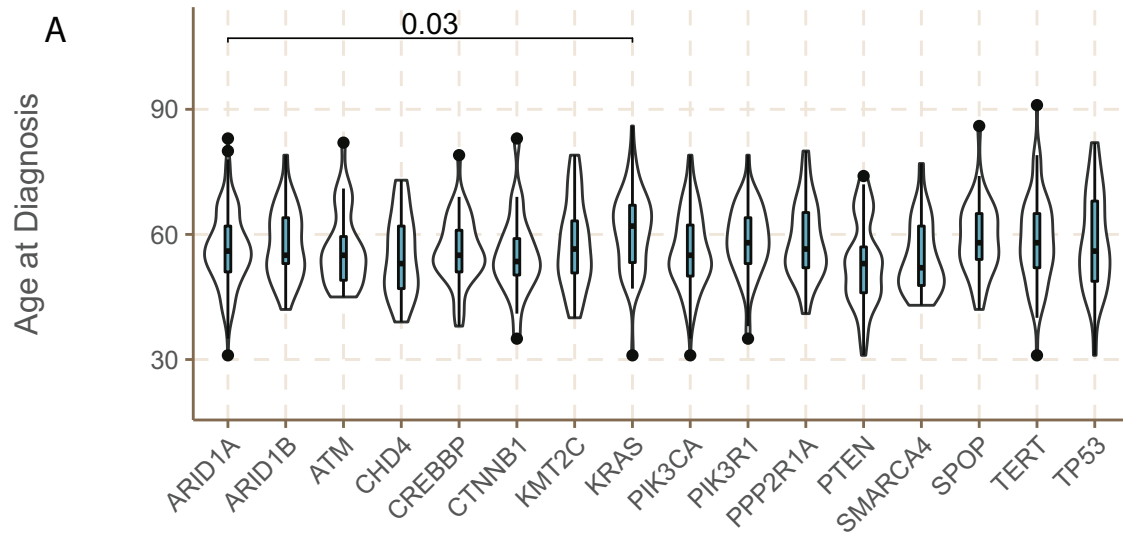


Figure 2

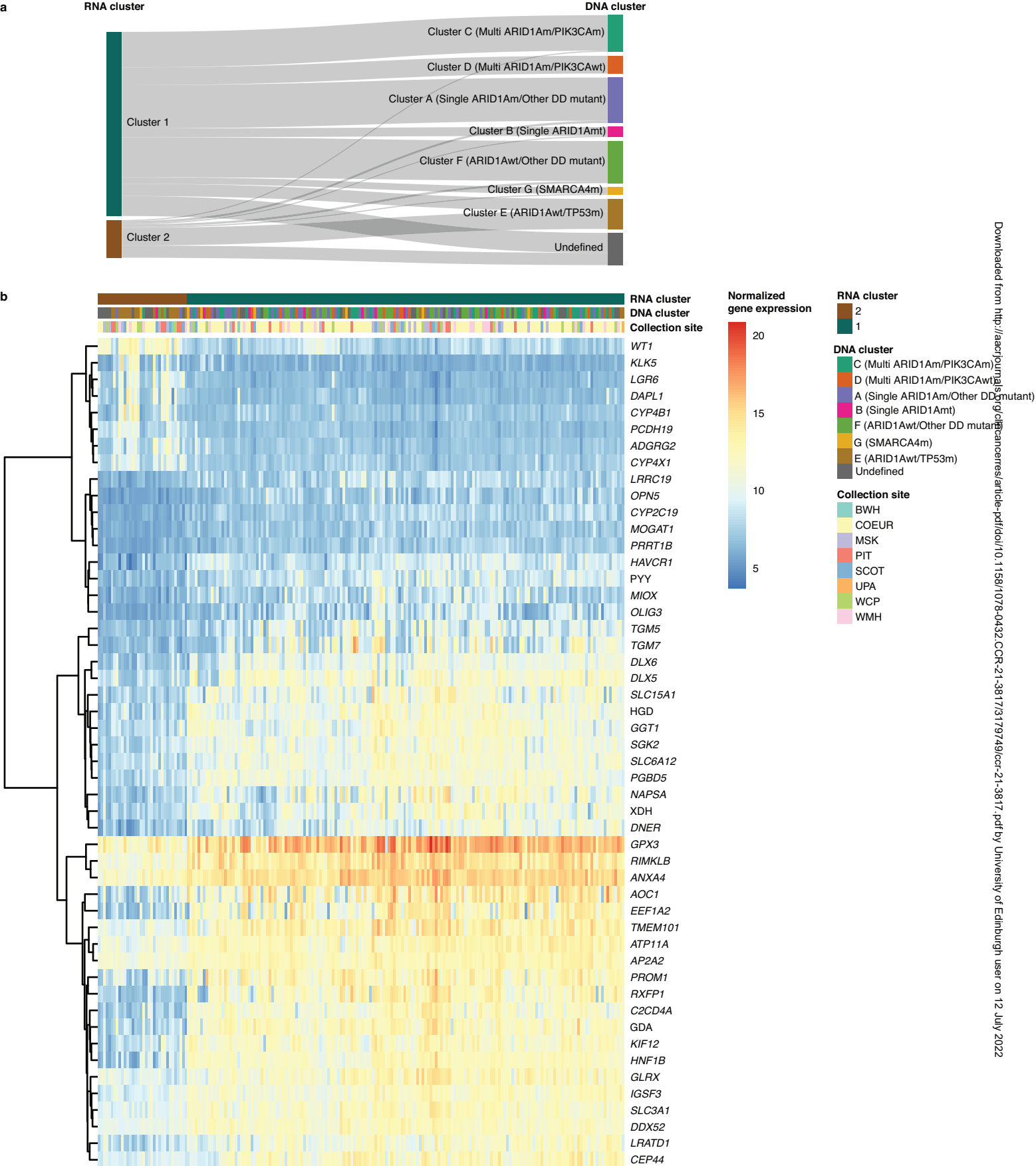
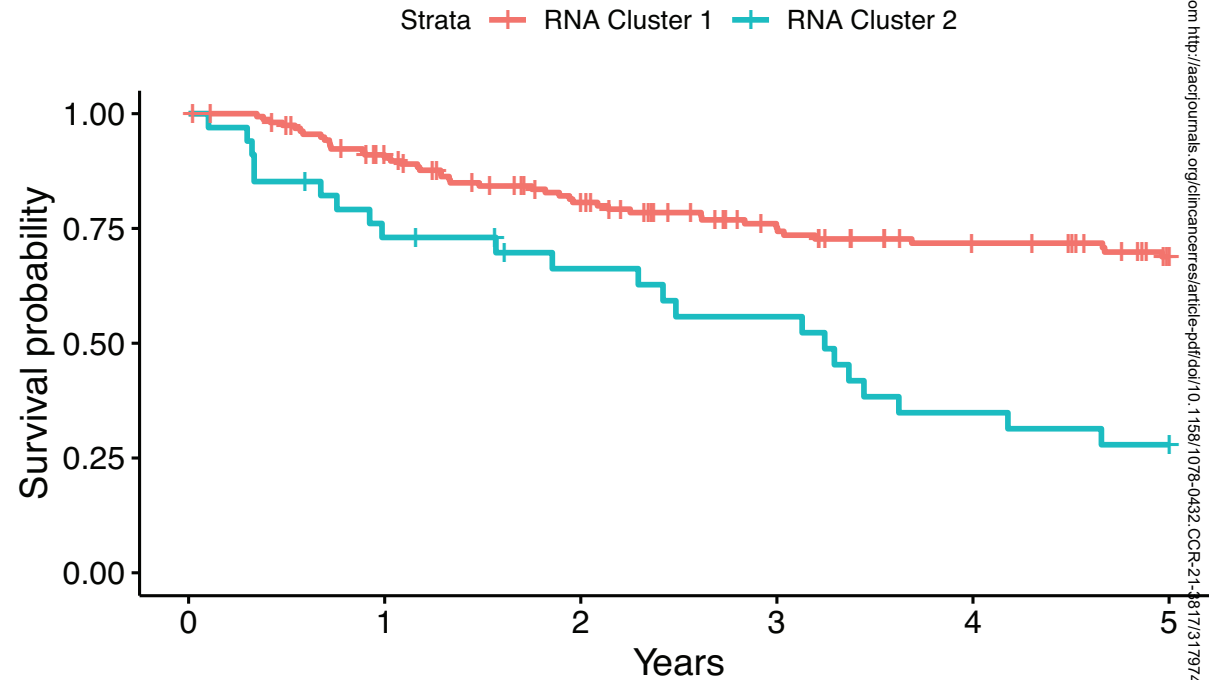
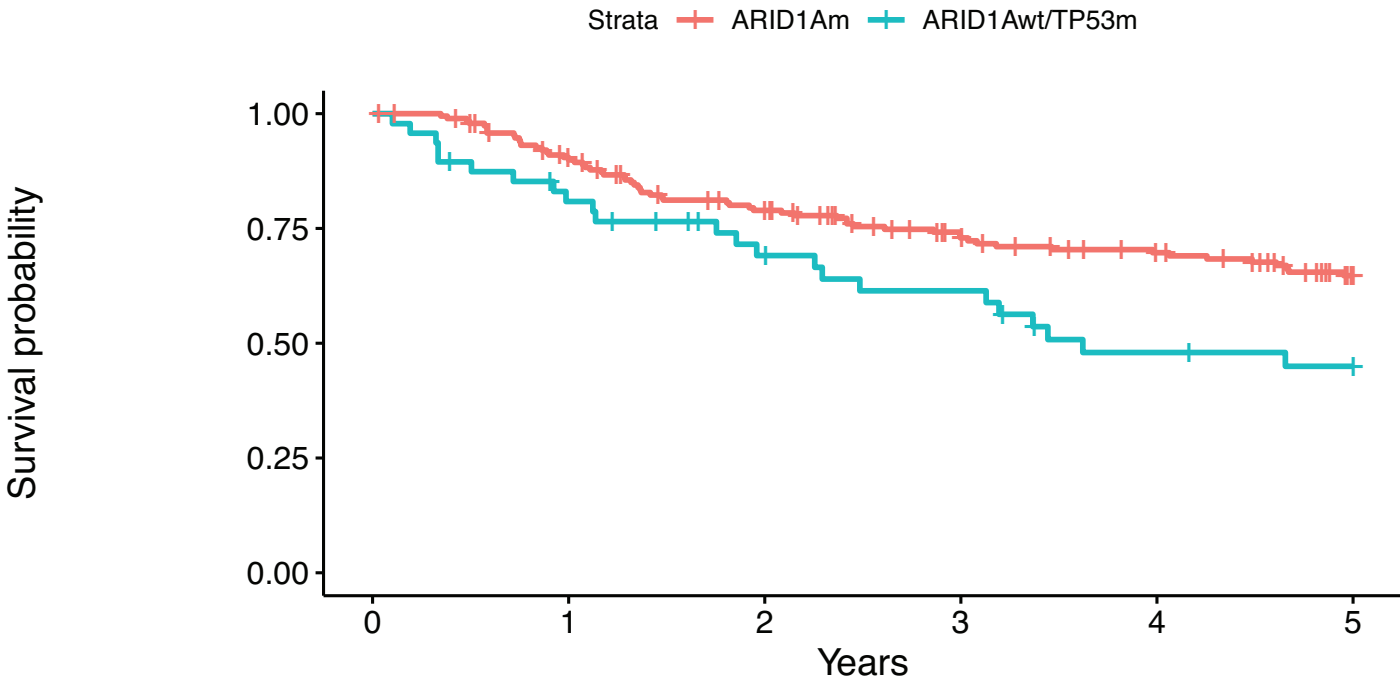


Figure 3



Number at risk

	Strata	ARID1Am	ARID1Awt/TP53m
ARID1Am	178	168	141
ARID1Awt/TP53m	46	37	28
	0	1	2
			3
			4
			5

Number at risk

	Strata	RNA Cluster 1	RNA Cluster 2
RNA Cluster 1	141	137	112
RNA Cluster 2	33	24	19
	0	1	2
			3
			4
			5

Figure 4